预应变下高强结构钢低温断裂性能

肖光春[1,2]，　荆洪阳[1,2]，　徐连勇[1,2]，　冀晋川[3]，　李文亮[3]
（1. 天津大学 材料科学与工程学院，天津　300072；2. 天津市现代连接技术重点实验室，天津　300072；
3. 山西电力科学研究院，太原　030001）

肖光春

摘　要：为了测试高强结构钢Q420力学性能和断裂韧度，对其原材料和塑性变形材料分别进行了不同温度下的拉伸试验和断裂韧性试验. 结果表明，结构钢的断裂韧性随着温度的降低显著减小，使其倾向于脆性断裂；而预应变虽然提高了钢材的屈服强度与抗拉强度，但显著降低了钢材的塑性及断裂韧性，进一步增加了脆性断裂发生的可能性. 同时利用有限元分析得出，预应变对延性断裂向脆性断裂转变的促进作用源于预应变引起裂纹尖端应力场的增大. 在重要工程设计、选材、安全分析及评定时，应充分考虑温度和预应变对结构断裂行为的影响.

关键词：高强结构钢；预应变；力学性能；断裂韧性
中图分类号：TG115.5　　**文献标识码**：A　　**文章编号**：0253-360X(2011)03-0041-04

0　序　言

钢结构因其具有良好的力学性能、经济性能和使用性能等优点，在工业厂房、桥梁、大型工业设备和高层建筑等领域得到广泛地应用. 但结构钢材的塑性和断裂韧性随着温度的降低而下降，构件的断裂行为也由韧性断裂向脆性断裂发生转变. 在低温环境下，即使在低应力下也会容易发生脆性破坏. 脆性断裂的发生具有突发性，事先毫无征兆，破坏过程瞬间发生，根本来不及采取补救措施，从而大大增加了钢结构破坏的危险性.

以往国内钢结构普遍采用Q235和Q345强度等级的钢材，与国外先进水平(Q450及以上)相比，强度偏低，结构用钢量偏大，增加了建设投资. 近年来，国内采用了生产技术较成熟、强度等级更高的Q420高强结构钢. 但在大量的工程建设过程中，结构钢材不可避免会承受大的塑性变形，即钢结构在使用前已经产生了一定塑性变形(即为预应变). 预应变的产生会直接影响钢结构的变形能力和断裂抗力，引起材料断裂韧性的下降，甚至会引起裂纹尖端的应力集中，导致脆性断裂的发生[1,2]，使钢结构失效的几率大增. 因此，在钢结构的断裂评定中必须考虑预应变对材料变形和断裂行为的影响.

国内外曾发生过许多钢结构破坏事故，造成了很大的经济损失和人员伤亡. 钢结构的破坏一般不是单一因素引起的，往往是多个因素综合作用的结果. 目前，国外主要对管道用钢进行了预应变下的低温断裂研究[1-3]. 对于结构钢，国内外少有研究. 文中主要对国内目前普遍采用的高强结构钢Q420原材料及具有一定预应变水平材料进行了低温断裂试验研究，分析了温度和预应变对其断裂韧性的影响，为钢结构的工程设计及应用提供依据.

1　试验方法

1.1　试验材料及其力学性能

试验用材选取典型建筑高强结构钢Q420角钢，规格为200 mm(支宽)×16 mm(厚度)，热处理状态为控轧+控冷. 该材料的化学成分如表1所示.

表1　Q420钢的化学成分(质量分数，%)
Table 1　Chemical composition of Q420 steel

C	Mn	Si	P	S	V	Cr
0.15	1.52	0.32	0.033	0.028	0.048	0.18

拉伸试验试样的取样方向均为纵向取样. 根据

收稿日期：2010-05-18
基金项目：国家自然科学基金资助项目(50975196)；教育部博士点新教师基金(20070056096)；高等学校博士学科点专项科研基金资助项目(20090032110026)；天津市自然科学基金资助项目(08JCYBJC09100)

图1所示的室温条件下原材料的应力—应变曲线，文中对2%预应变水平进行了分析研究. 由于预应变下的真应力—真应变曲线几乎遵循原材料的应力—应变曲线，因此，预应变下的屈服强度 R_{eLp} 等于原材料在真应变 ε_{pre} 时的真应力，其抗拉强度 R_{mp} 可以通过以下公式[4]计算得到，即

$$R_{mp}=\frac{1+\varepsilon_T}{1+\varepsilon_T-\varepsilon_{pre}}\cdot R_m \qquad (1)$$

$$\varepsilon_{Tp}=\varepsilon_T-\varepsilon_{pre} \qquad (2)$$

式中: ε_{Tp} 和 ε_T 分别为预应变材料和原材料在最大载荷时的工程应变; R_m 为原材料的抗拉强度. 其中，ε_{Tp} 随着预应变的增大而减小. 原材料及2%预应变水平材料的拉伸试验结果见表2. 由此可见，预应变提高了材料的屈服强度和抗拉强度，而降低了塑性. 此外，预应变对屈服强度的影响程度大于对抗拉强度的影响程度.

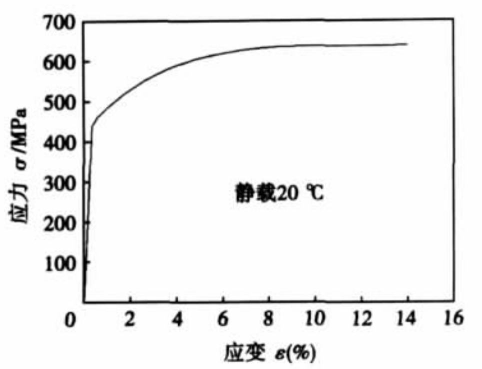

图1 Q420 结构钢应力—应变曲线

Fig. 1 Nominal stress-strain curve of Q420 steel

表2 Q420 结构钢的拉伸力学性能

Table 2 Mechanical properties of Q420 steel

Q420	温度 T/℃	屈服强度 R_{eL}/MPa	抗拉强度 R_m/MPa
	20	440	638.3
$\varepsilon_{pre}=0$	0	450	661
	-20	460	685
	20	531	650
$\varepsilon_{pre}=2\%$	0	542	671
	-20	554	690

1.2 CTOD 试样制备

CTOD预应变试样的制备过程如下. 首先由Q420角钢加工成如图2所示的板状拉伸试样，然后在300 kN的万能材料试验机上进行预应变拉伸处理，当每个试样的工程应变达到预定的 e 时停止加载，则残余预应变 ε_{pre} 可以通过式(3)进行计算，即

$$\varepsilon_{pre}=\ln(1+e) \qquad (3)$$

文中取2%预应变水平进行研究，最后从拉伸预应变试样(图2)的平行部分的中心处截取材料，并加工成如图3所示的符合英国标准BS7448[5]:1991—Part Ⅰ的三点弯曲(SEB)标准试样. 没有预应变的CTOD试样直接从角钢上纵向截取加工成标准CTOD试样. 试样缺口采用直径为0.10 mm的钼丝线切割11 mm长度缺口后，再用高频疲劳试验机预制2 mm长度的疲劳裂纹模拟实际工程中的初始尖锐裂纹. 在预制疲劳裂纹过程中，应控制裂纹扩展不要太快以免裂纹尖端发生塑性变形，制备试样的最终裂纹深度与板宽之比控制在0.45～0.55，具体试样尺寸如图3所示.

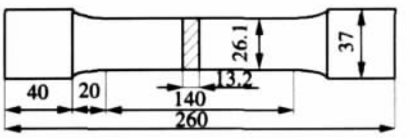

图2 拉伸预应变试样(mm)

Fig. 2 Tensile prestraining specimen

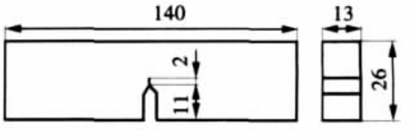

图3 Q420 结构钢 CTOD 试样尺寸(mm)

Fig. 3 CTOD specimen of Q420 steel

2 试验过程及结果分析

2.1 试验过程

断裂试验是在300 kN的万能材料试验机上进行，试验过程中通过电脑软件自动记录 F-V 曲线(F 为施加载荷，V 为试样裂纹嘴张开位移)并存储试验数据. 整个试验步骤如下.

(1) 对每个试样测量其厚度 B、宽度 W 及刀口厚度 z，测量精度为0.02 mm.

(2) 试验之前对载荷、位移测量系统进行标定，标定过程在室温条件下进行.

(3) 将试样放在盛有干冰、酒精低温介质的低温槽中进行冷却. 试验温度分别为 -20，0和20 ℃，应保证测温计距裂纹尖端不超过2 mm范围，精度为±2 ℃，保温时间为每毫米不少于30 s(试验跨距 S 为 $4W\pm0.2W$，实际记录跨距时偏差为±0.5%).

(4) 采用一次加载的方式直到试样失稳破坏，加载速率 K 在线弹性变形时应保证在0.5～3.0

$MPa \cdot m^{0.5}/s$ 之间，并同时记录试样载荷—位移曲线. 需要注意的是试样加载到 F–V 曲线达到最大载荷并刚刚开始下降时卸载，或试样发生脆断失稳破坏时立刻开始卸载.

(5) 试样失稳破坏后，从低温槽中取出，对断口进行烘干处理后在试验机上快速压断试样. 从断裂试样上取下断口形貌用工具显微镜测量试样的初始裂纹长度的平均值 a_0 和裂纹长度的平均值 a，由此计算出裂纹扩展量 $\triangle a$. 测量的具体方法为沿试样厚度方向取 9 个测量位置分别进行测量(图 4)，其中最外侧的两个点位于距试样表面 1% B 处，然后在这两个点之间等间距的取 7 个测量位置. 裂纹长度按下述公式计算，即

$$a_0 = \frac{1}{8}\left(\frac{a_{01} + a_{09}}{2} + \sum_{i=2}^{8} a_{0i}\right) \quad (4)$$

$$a = \frac{1}{8}\left(\frac{a_1 + a_9}{2} + \sum_{i=2}^{8} a_i\right) \quad (5)$$

$$\triangle a = a - a_0 \quad (6)$$

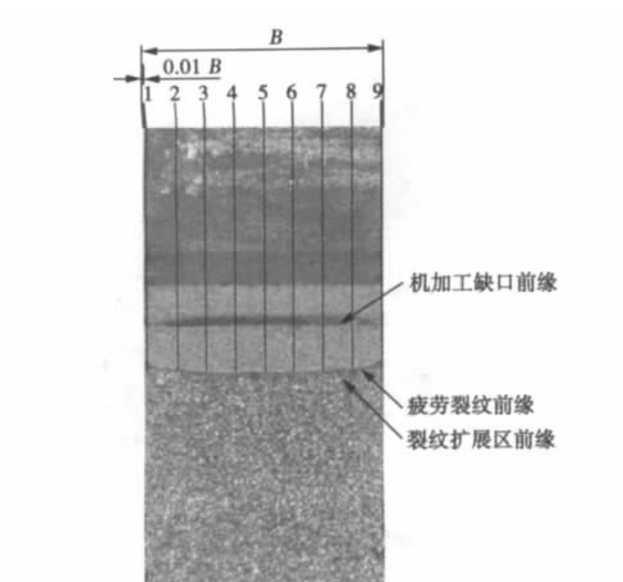

图 4　CTOD 试样裂纹长度的测量

Fig. 4　Crack length measure of CTOD specimen

(6) 数据处理. 根据 F–V 曲线上的最大载荷 F (N) 和对应最大载荷时的塑性张开位移 V_P (mm) 按 BS7448 Part Ⅰ中的下述式(7)计算 CTOD 值，即

$$\delta_0 = \left[\frac{FS}{BW^{1.5}} \times f\left(\frac{a_0}{W}\right)\right]^2 \frac{(1-\upsilon^2)}{2R_{eL}E} + \frac{0.4(W-a_0)V_p}{0.6a_0 + 0.4W + z} \quad (7)$$

式中：弹性模量 $E = 2.01 \times 10^5$ MPa；泊松比 $\upsilon = 0.3$；R_{eL} 为材料屈服强度；$f(a_0/W)$ 为几何形状因子，可根据 a_0/W 的数值直接查表得到.

(7) 有效性判别. BS7448 标准对母材金属有效试样规定如下：平均裂纹长度为 $a_0 = 0.45 \sim 0.55\ W$；裂纹前缘任意两个裂纹长度差值均不大于 10% a_0.

2.2　试验结果及其分析

典型的载荷—位移曲线如图 5 所示，曲线上最大载荷处的拐点即为试样发生失稳断裂破坏时刻. 通过计算得到的 Q420 原材料和 2% 预应变试样在不同温度下的 CTOD 值，如图 6 所示. 由图 6 可以清楚地看到，温度对结构钢的断裂韧性有明显的影响，随着温度的降低钢材的断裂韧性显著减小，使钢材由延性断裂向脆性断裂转变. 在同一个温度下，预应变的存在也显著降低了钢材的断裂韧性，进一步促进了脆性断裂的发生. 因此，具有一定塑性预应变的钢结构在低温环境下具有低的安全性，极易发生脆性断裂破坏.

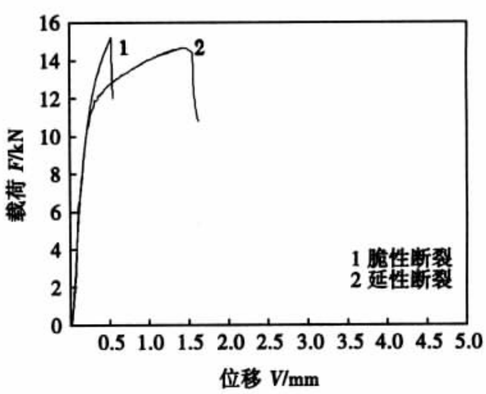

图 5　典型的载荷—位移曲线

Fig. 5　Typical load-displacement curve

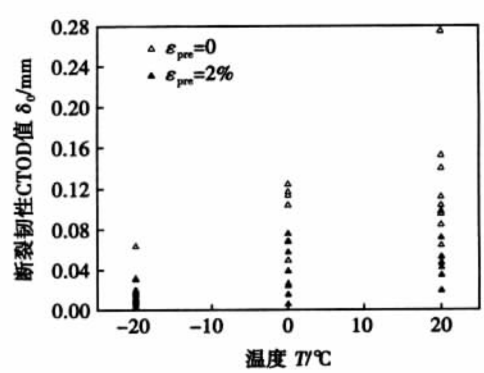

图 6　Q420 不同温度下的 CTOD 值

Fig. 6　CTOD values under different temperatures

3　有限元分析

裂纹尖端周围的应力场对断裂韧性特性具有重要的作用[4,6]. 采用 ABAQUS Ver. 6.9-1 三维有限

元软件分析了预应变对 CTOD 试样裂纹尖端应力场的作用. 由于采用有限元计算的三点弯曲试样具有对称性,取试样的 1/4 建模(图 7) ,采用八节点六面体线性减缩积分单元. 裂纹尖端最小尺寸为 0.002 mm ×0.005 mm ×0.04 mm,其局部网格划分如图 7b 所示,共分 8 590 个单元、10 854 个节点. 采用裂纹尖端张开位移 CTOD 表征裂纹尖端的载荷水平.

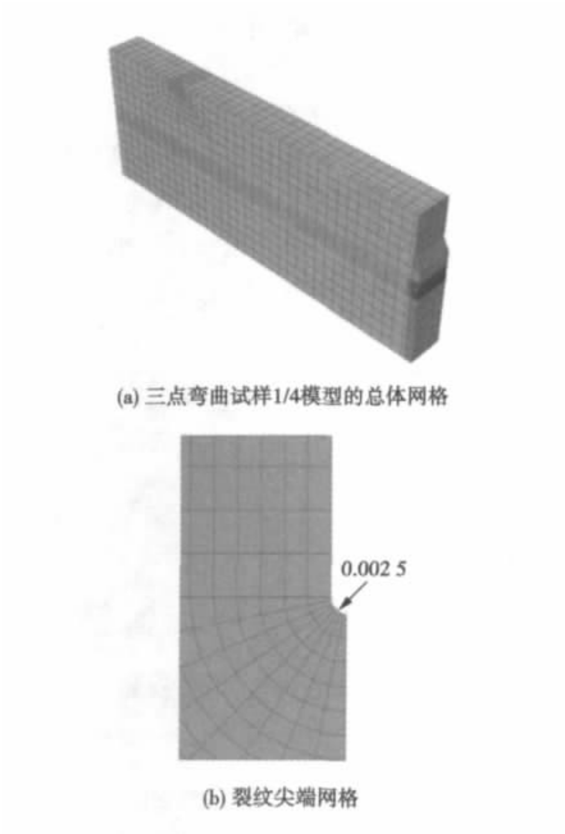

(a) 三点弯曲试样1/4模型的总体网格

(b) 裂纹尖端网格

图 7 三点弯曲试样有限元计算模型

Fig. 7 Finite element calculation model for three-point bending specimen

图 8 给出了在相同温度下发生一定变形水平时

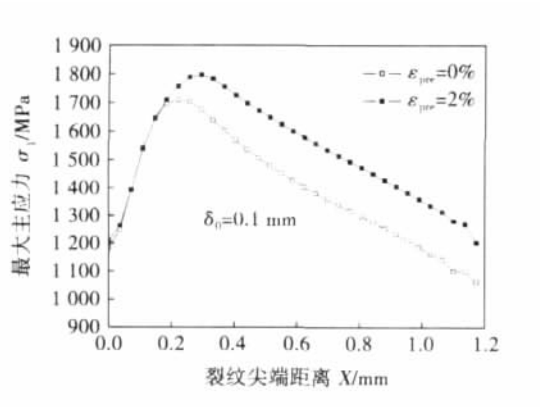

图 8 预应变对裂纹尖端应力场的影响

Fig. 8 Effect of prestrain on stress fields near crack tip of CTOD specimen

(δ_0 =0.1 mm) 两种 CTOD 试样板厚中部裂纹尖端区域最大主应力 σ_1 的分布,由图 8 可见裂纹尖端区域的应力由于预应变而升高. 对于其它温度情况,也有相同的趋势. 这就定性说明了预应变对裂纹尖端区域应力的这种增大作用促进了 CTOD 试样由延性断裂向脆性断裂的转变.

4 结 论

(1) 温度对结构钢的断裂韧性有明显的影响,随着温度的降低,钢材的断裂韧性显著减小,使钢材由延性断裂向脆性断裂转变.

(2) 预应变提高了钢材的屈服强度与抗拉强度,但显著降低了钢材的断裂韧性,进一步增加了发生脆性断裂的可能性. 在重要工程设计、选材、安全分析及评定时,应同时考虑预应变作用的影响.

(3) 通过有限元软件对断裂过程模拟分析得出,预应变的存在引起裂纹尖端区域应力场的增大,这种作用促进了 CTOD 试样由延性断裂向脆性断裂的转变.

参考文献:

[1] Hagiwara N, Masuda T, Oguchi N. Effects of prestrain on fracture toughness and fatigue-crack growth of line pipe steels[J]. Journal of Pressure Vessel Technology, Transaction of the ASME, 2001, 123: 355 – 361.

[2] Fukuda N, Hagiwara N, Masuda T. Effect on prestrain on tensile and fracture toughness properties of line pipes[J]. Transaction of the ASME, Journal of Offshore Mechanics and Arctic Engineering, 2005, 127: 263 – 268.

[3] Sivaprasad S, Tarafder S, Ranganath V R, *et al*. Effect of prestrain on fracture toughness of HSLA steels[J]. Materials Science and Engineering A, 2000, 284: 195 – 201.

[4] Minami F, Arimochi K. Evaluation of prestraining and dynamic loading effects on the fracture toughness of structural steels by the local approach[J]. Journal of Pressure Vessel Technology, 2001, 123(3) : 362 – 372.

[5] BSI. Part 1: method for determination of KIC, critical CTOD and J values of metallic materials BS 7448 [S]. London: BSI Publictaions, 1991.

[6] Eikrem P A, Zhang Z L, Nyhus B. Effect of plastic prestrain on the crack tip constraint of pipeline steels[J]. Pressure Vessels and Piping, 2007, 84: 708 – 715.

作者简介: 肖光春,男,1979 年出生,博士研究生. 主要从事焊接结构强度及断裂方面的研究. 发表论文 4 篇. Email: xgc@ tju. edu. cn na). p 37 – 40

Abstract: Ultra-assisted electrode sparkle depositing (UAESD) developed based on the traditional electrode sparkle depositing (ESD), and better coating could be achieved when ultrasonic vibration was adopted in the ESD technology. In this paper, UAESD was realized by the supersonic vibration of the body. The results showed that formation technological parameters were enlarged by supersonic vibration, and the better surface topography was achieved. The deposition efficiency increased 30%, microhardness increased 10% while the grain size decreased 24.18% under the influence of the supersonic vibration. With the UAESD process, heat affected zone was enlarged and the microhardness at those points was increased. Moreover, the corrosion resistance of the bond was enhanced.

Key words: supersonic vibration; electrode sparkle depositing; strengthen coating

Research on fracture toughness of high-strength structural steel with prestrain at low temperature XIAO Guangchun[1,2], JING Hongyang[1,2], XU Lianyong[1,2], JI Jinchuan[3], LI Wenliang[3] (1. School of Materials Science and Engineering, Tianjin University, Tianjin 300072, China; 2. Tianjin Key Laboratory of Advanced Joining Technology, Tianjin 300072, China; 3. Shanxi Electric Power Research Institute, Taiyuan 030001, China). p 41 – 44

Abstract: The mechanical properties and fracture toughness of high-strength structural steel Q420 were studied by tension tests and three-point bending tests. The results indicated that the temperature had significant influence on fracture toughness of structural steel and the fracture toughness reduced significantly with the decrease of temperature resulting in brittle fracture. The prestrain increased the yield strength and tensile strength of structural steel, but significantly reduced its plasticity and fracture toughness, and further increased the possibility of brittle fracture. The prestrain facilitated the brittle fracture due to the activation of the near crack tip stress fields because of the prestrain based on the FEA. Thus the effects of the temperature and the prestrain should be considered in the important engineering design, material selection, safety analysis and evaluation.

Key words: high-strength structural steel; prestrain; mechanical properties; fracture toughness

Microstructure transformation and mechanical properties of electron beam welded joints of fusion CLAM steel JIANG Zhizhong[1], HUANG Jihua[1], CHEN Shuhai[1], JU Xin (1. School of Materials Science and Engineering, University of Science & Technology of Beijing, Beijing 100083, China; 2. School of Applied Science, University of Science & Technology of Beijing, Beijing 100083, China). p 45 – 48

Abstract: China low activation martensitic (CLAM) steel for fusion reactor were butt-welded through electron beam welding process, and followed by post-welding heat treatment (PWHT) at 740 ℃ for 1 h. The microstructure and microhardness distribution of welded joints were analysed. The results showed that the weld seam with good formation and without appearance defects has been achieved. In as-welded condition, the weld metal and fusion zone consisted of a mixture of coarse lath martensite and a little δ ferrite. The coarse and fine grained zone was composed of fine lath martensite. The partially quenched zone mainly consisted of fine lath martensite and ferrite. The softening did not occur across welded joint. After PWHT, the lath martensite in the welded joint was transformed into tempered sorbite, which led to the significant decrease of the hardness of each zone. Among them, the highest hardness emerges at fusion zone was not at fine grained zone, which was just 20% higher than base metal. The PWHT did not make the tempered zone and base metal more soft obviously.

Key words: China low activation martensitic steel; electron beam welding; microstructure; microhardness

Influence of magnetic controlled technology on formation of high-speed TIG welding CHANG Yunlong[1], YANG Dianchen[1], WEI Lai[1], LU Lin[2] (1. Department of Material Science and Engineering, Shenyang University of Technology, Shenyang 110023, China; 2. Chemical Equipment College, Shenyang University of Technology, Liaoyang, Liaoning 111003, China). p 49 – 52

Abstract: Increasing TIG welding speed may raise productivity. Welding speed increasing, however, will cause arc dragged backwards and anode spot delayed seriously. The two phenomena generate the defects of undercut and hump seam. As usual, the method of augmenting the shielding gas feed rate or increasing welding current was chosen to achieve it, but the abilily to increase the welding speed was limited. The influence of transverse magnetic field on the welding speed, welding current and argon flow of high-speed TIG welding for austenite stainless steel were studied. The microstructure observation and flaring test were ivestigated. The experiment results indicated that welding speed could be increased from 3.5 m/min to 5.5 m/min, at the same time, welding current could be decreased from 95 A to 75 A, gas feed rate could be reduced from 0.7 m^3/h to 0.5 m^3/h, and the problems of undercut and hump seam due to high-speed TIG welding could be well solved.

Key words: high-speed TIG welding; magnetic field; undercut; flaring test

Microstructures and mechanical properties of Co-based surfacing alloys under DC transverse magnetic field LIU Changjun[1], LIU Zhengjun[2], SU Ming[2], SU Yunhai[2] (1. School of Chemical Equipment, Shenyang University of Technology, Liaoyang, Liaoning 111003, China; 2. School of Material Science and Engineering, Shenyang University of Technology, Shenyang 110870, China). p 53 – 56, 60

Abstract: In order to improve the properties of surfacing layers, study the influence of surfacing current and magnetic field current on properties and microstructure of surfacing layer, DC transverse magnetic field was applied when Co-based alloy was welded on the surface of low-carbon steel by plasma arc surfacing. The hardness, wear resistance, microstructure and phase constitution of the surfacing layers were investigated via hardness and wear tests as well as SEM and XRD analysis. Furthermore, the influence of surfacing current and magnetic field current on the hardness and wear resistance of the surfacing layer were studied. The results showed that the properties of surfacing layers